MOMENTUM COLLIMATION IN A HIGH-INTENSITY COMPACT RAPID CYCLING PROTON SYNCHROTRON

J.Y. Tang#, J.F. Chen, Y. Zou, IHEP, Beijing 100049, China

Abstract:

Momentum collimation in a high intensity RCS is a very important issue. Based on the two-stage collimation principle, a combined momentum collimation method is proposed and studied here. The method makes use of the combination of secondary collimators in both the longitudinal and transverse planes. The primary collimator is placed at a high-dispersion location of an arc, and the transverse and longitudinal secondary collimators are in a dispersion-free long straight section and in an arc, respectively. The particles with a positive momentum deviation will be scattered by a Carbon scraper and then cleaned by the transverse collimators, whereas the particles with a negative momentum deviation will be scattered by a Tantalum scraper and mainly cleaned by the longitudinal secondary collimators. This is due that a Carbon foil produces relatively more scattering than a Tantalum foil if the energy loss is kept the same. The relevant requirements on the lattice design are also discussed, especially for compact rings. The multi-particle simulations using both TURTLE and ORBIT codes are presented to show the physical images of the collimation method, with the input of the CSNS RCS ring.

INTRODUCTION

For high intensity proton synchrotrons, collimation systems are needed, not only to intercept particles that are outside prescribed betatron and momentum acceptances, but also to trap these particles with high efficiency. In this paper, the emphasis is on the momentum collimation for a high-intensity compact rapid cycling proton synchrotron.

For large synchrotrons such as LHC at CERN and main injector in FERMILAB, there are sufficient spaces to allocate a full two-stage momentum collimation system in one of the arcs [1-3]. However, for compact synchrotrons, the straight sections in arcs are much limited and there is no sufficient space to host a full two-stage momentum collimation system. Thus, simplified momentum collimation method is employed for the latter case. The two reference methods are: the ISIS method by using two-stage massive collimators [4]; the J-PARC method by using a standard two-stage collimation but with the secondary collimators in the downstream dispersion-free straight section [5]. The former has the two collimators within the same long dispersive straight section, and the latter has the primary collimator in one of the arc sections and shares the secondary collimators with the transverse collimation system. The new momentum collimation method proposed here will be a combined collimation method: it will be a full two-stage collimation method, but with secondary collimators in one arc straight sections and one dispersion-free straight section. We take the CSNS/RCS as the example to study the collimation mechanism, but the method is general and applicable to other similar machines.

The China Spallation Neutron Source (CSNS) of several hundreds KW is to be constructed in Dongguan, Guangdong Province, China [6-7]. It is a short-pulse accelerator facility mainly consisting of an H^- linac and a proton rapid cycling synchrotron (RCS). The facility will be constructed in three phases (CSNS-I for 100 kW, CSNS-II for 200 kW, and CSNS-II for 500 kW, see Table 1.

Table 1：Main Parameters of CSNS

	CSNS-I	CSNS-II	CSNS-III
Beam power (kW)	100	200	500
Repetition rate (Hz)	25	25	25
Average current (μA)	62.5	125	312.5
Linac beam energy (MeV)	80	130	250
Proton energy (GeV)	1.6	1.6	1.6
RCS accumulated particles	1.6×10^{13}	3.2×10^{13}	7.8×10^{13}

MOMENTUM COLLIMATION SCHEME

Combined Method for Momentum Collimation

The CSNS/RCS lattice of four-fold and all-triplet cells [8] has been designed to provide good conditions to place momentum collimators, with a high normalized dispersion at the middle points of the arcs that is good place the primary momentum collimator and sufficient space in the same straight section to place a secondary collimator.

The combined scheme for momentum collimation in the RCS for all the CSNS phases is detailed here: 1) Make use of the all-triplet lattice. 2) Using a thin Tantalum foil at negative momentum deviation (or negative X) to produce significant scattering but with little energy loss, this can help minimizing the decrease in Courant-Snyder invariant (or I_x) due to the longitudinal-horizontal coupling effect. 3) Using a thin Carbon foil at positive

tangjy@ihep.ac.cn

momentum deviation (or positive X) to produce significant increase in I_x when keeping a modest scattering. 4) Using a thick Nickel (or copper or Inconel) block as a secondary collimator along with the thin foil but at the negative X position of 0.5 mm further from the optical axis. The betatron motion in turns can make the collimator effective in removing the scattered particles but still having small I_x. This collimator can also act as a single-stage collimator to absorb the particles with very large momentum deviation and with a large momentum precession at the same time. 5) A second thick collimator located in the downstream arc section to localize some of the lost particles scattered in the vertical phase plane, in order to reduce beam losses in the magnets before reaching the transverse collimators. 6) The whole transverse collimation system in the dispersion-free straight section will be employed to collimate the scattered or energy-lowered particles by the momentum collimators. Figure 1 shows the lattice functions and the momentum collimation scheme. Parameters of the collimation system are given in Table 2.

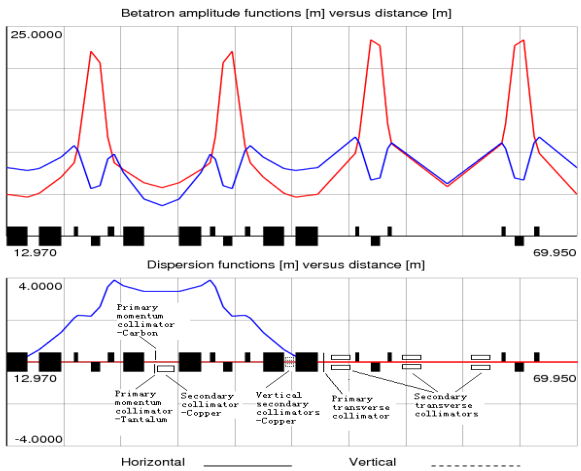

Figure 1: Triplet lattice and the momentum collimation scheme for CSNS/RCS

Table 2：Parameters of the Collimators

Collimators	**Primary**		**Secondary**	
Materials	Ta foil	C foil	Cu block	Cu block
Long. Pos. (m)	28.465	28.465	28.515	40.910
Thickness (mm)	0.002	0.05	50	50
Shape	Erect	Erect	Erect	Erect
Transverse pos.	-X	+X	±X	±Y
Off axis (mm)	-71.08	+71.08	±71.08	±45.66

Longitudinal-transverse Coupling Effect

As mentioned in Ref. [9-10], the energy loss in a thin primary collimator at dispersive locations with positive momentum deviation will increase I_x in betatron motion, which is helpful for the collimation of those particles in the dispersion-free straight. In the contrary, it will decrease I_x if the momentum deviation is negative and thus is not favoured. The Courant-Snyder invariant change can be expressed by:

$$\Delta I_{x,p} = 2D_n \sqrt{I_x} \frac{\Delta p}{p_0}$$

where $I_x, D_n, \Delta p / p, \Delta I_{x,p}$ are original Courant-Snyder invariant, normalized dispersion and change in Courant-Snyder invariant.

Figure 2 shows that a hollow beam with a positive momentum deviation passed through a primary collimator has an increased I_x at a place in dispersion-free region, and scattering effect is also included.

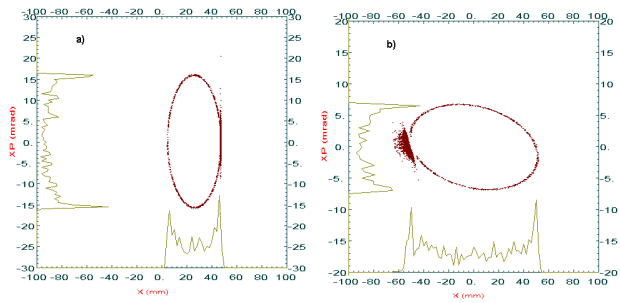

Figure 2: Longitudinal-transverse coupling effect in a primary momentum collimator (a: at the scraper; b: at a dispersion-free location; Triplet lattice, carbon foil: 0.05 mm, E: 80 MeV, δ: 1.0%)

Material Choice for Primary Momentum Collimator

Material choice for the primary momentum scraper is important here. We can find that different materials have different effect in energy loss and scattering angle. For different materials but the same rms scattering angle, the relative change in momentum due to the passing thru the foil is different. For material of higher atomic number, the relative change in momentum is smaller. For example, the relative momentum loss is only one seventh in Tantalum than in Carbon, e.g. 1.0×10^{-4} and 7.3×10^{-4} at 80 MeV, respectively, and this rule holds for different beam energy. Therefore, a Tantalum foil is chosen at negative X and a Carbon foil is chosen at positive X for the primary collimators to play the corresponding roles. Besides, it is necessary that a thick block will be used to absorb particles with relatively large impact depth for the secondary collimators.

Material Choice for Secondary Momentum Collimator

As the thick collimator at arc acts also as the one-stage momentum collimator, when the impact parameter is large, materials with high stopping power and low scattering effect are favoured to obtain high collimation efficiency. In theory, to have a short stopping range and a small scattering angle per unit length, a material of large density and low-Z is helpful. The elements or their alloys in Column VIII in the Periodic Table of the Elements look to be good candidates, e.g. Nickel-base alloy Inconel or copper.

Beam Correlation and Collimation

One can fill the beam emittance in an RCS by correlated or anti-correlated injection painting [11]. When the particles with larger momentum deviation passes through a primary momentum collimator placed at larger X position, the correlation will play an important role in the vertical plane. If the beam is anti-correlated, when the inner particles in the horizontal emittance with a large negative momentum deviation are to be collimated, they have a large I_y. This means that the scattering is perhaps too strong in the vertical plane and results in significant beam loss in the rest of arc, as shown in Figure 3. The similar situation happens at collimating the particles with large I_x and I_y when the beam is correlated. Detailed studies are needed to determine which one is better.

As we do not hope that any particle hits the primary momentum collimators due to the vertical betatron motion, erect collimators instead of inclined or elliptical ones will be used here.

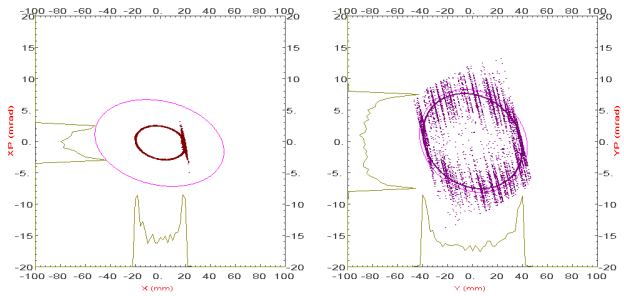

Figure 3: Beam distributions at the primary transverse collimator (TURTLE simulation; anti-correlated beam; energy: 80 MeV; primary Ta collimator thickness: 0.0013 mm; ellipses in pink are for the acceptance of the transverse collimation)

SIMULATION RESULTS

In order to demonstrate the collimation effect of the combined momentum collimation method, single-pass simulations by using TURTLE [12] have been carried out at first. It confirms the collimation mechanism as predicted by the theory. To analyze the correlation effect, hollow beams in phase spaces are produced by using a self-made FORTRAN program to represent either correlated or anti-correlated or non-correlated beams. This will also make the simulations much more efficiently with relatively less particles.

ORBIT code [13] is employed to study more realistic situations with both secondary momentum collimators and transverse collimators. The collimation is carried out in multi-turn mode including acceleration. Both hollow and filled beams are used in the simulations. To simplify the study, the transverse collimators are presented by a single black-body absorber but with a collimation efficiency of about 95% [14].

Assuming the particles to be collimated by the momentum collimation system first hit the primary momentum collimator, and then they are removed by the secondary collimators in successive turns. With the correlated beam, the scattering effects at the primary momentum collimator in both the horizontal and vertical planes are important, especially for those particles with large Ix and Iy. Thus, there is relatively more beam loss in the arc. With the anti-correlated beam, the scattering effect in the primary momentum collimator in the vertical plane is much less important for those particles with large Ix. Figure 4 shows the anti-correlated beam distributions with an off-momentum 1.03% at the second turn. Figure 5 shows the anti-correlated beam distributions with an off-momentum -1.03% and -1.85%, which are seen as beam halo and beam core in the horizontal plane, respectively

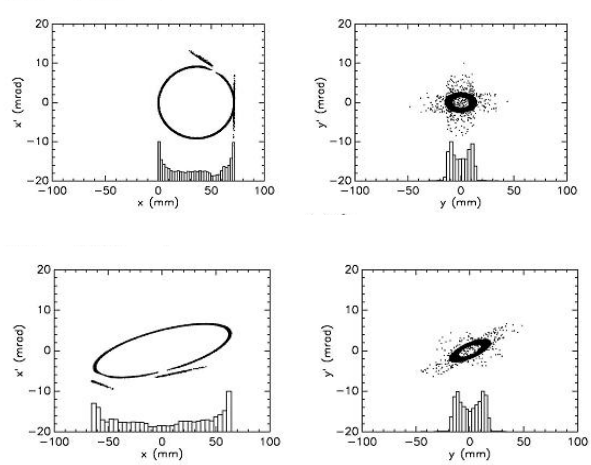

Figure 4: Beam distributions at the second turn (anti-correlated beam; energy: 80MeV; off-momentum: δ= 1.03%; upper: just after the primary momentum collimator; lower: just after the transverse black-body collimator in the straight section.)

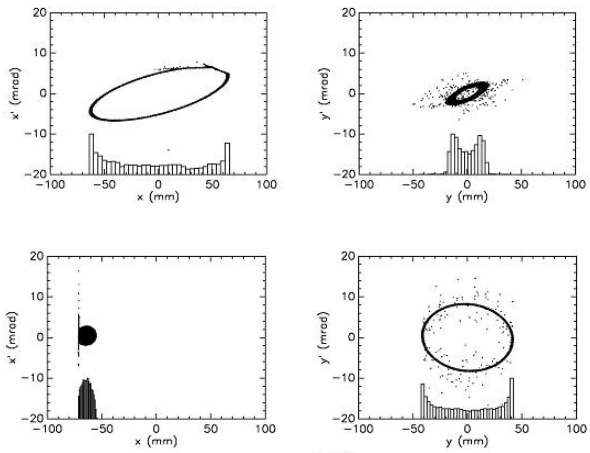

Figure 5: Beam distributions at the second turn (anti-correlated beam; energy: 80 MeV; upper: δ= -1.03%, seen as beam halo in horizontal plane, just after the transverse black-body collimator in the straight section; lower: δ= -1.85%, seen as beam core in horizontal plane, just after the primary momentum collimator.)

One of the advantages with this combined two-stage momentum collimation method is that it is almost independent of beam energy. When the RCS is upgraded with higher injection energy, we need only to replace the momentum scrapers by thicker ones. At the energy of 80 MeV, with a thickness of 0.05 mm for the Carbon scraper, the energy loss due to one pass in the scraper is equivalent to about 4.4×10^{-4} in relative momentum change, and this is low enough to allow a multi-turn collimation possible.

Table 3 shows the momentum collimation efficiencies and turns to remove almost all the particles of a hollow beam. Figure 6 gives the positions of the lost particles in the ring, where the injected beam contains 10000 particles and with -1.03% off-momentum (δ). The poor collimation efficiencies with larger I_y in both anti-correlated and correlated beams are due to the scattering in the vertical plane that results in beam losses in the arc magnets. On the one hand, this is due to the poor definition of the dipole vacuum chambers in elliptical shape instead of a more realistic race-track shape; on the other hand, a vertical collimator before the dipole just following the primary momentum collimator will help reduce the uncontrolled beam loss. Therefore, the simulations for the overall collimation efficiency are still under way.

Table 3: Collimation efficiencies and turns to collimate all the particles with the combined collimation method at energy level of 80 MeV

C-S invariant (πmm.mrad) /off- momentum	Anti-correlated		Correlated	
	Uncontr. beam loss	Turns	Uncontr. beam loss	Turns
Ix=333, δ= 1.03%	9.5%	210	90.8%	10
Ix=333, δ= -1.03%	6.3%	160	65.2%	60
Ix=298, δ= -1.16%	2.8%	100	64.0%	60
Ix=18, δ= -1.85%	78.3%	120	8.3%	170

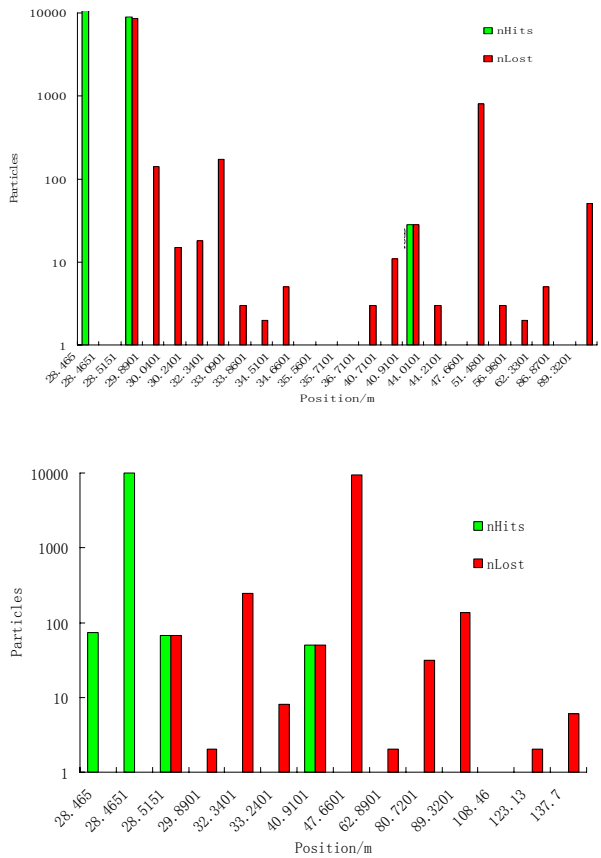

Figure 6: The relationship between the all lost particles and the corresponding positions in the ring with the combined collimation method, where nHits means the number of particles hitting on the collimators and nLost means the number of absorbed particles (anti-correlated beam; total 10000 particles injected; energy level: 80 MeV ; upper: δ= - 1.03%; lower: δ= 1.03%).

CONCLUSIONS

The simulation studies show that the combined scheme for momentum collimation in RCS is an effective method. The particles with large positive off-momentum pass through a thin Carbon foil, and will be removed mainly by the transverse collimation system. The particles with large negative off-momentum pass through a thin Nickel foil, and will be collimated mainly by the secondary momentum collimator. Beam correlation from the injection painting plays an important role in the momentum collimation, and the anti-correlated beam is favoured. More detailed study is under way.

ACKNOWLEDGEMENTS

The authors would like to thank CSNS colleagues, especially N. Wang for the discussions and helps.

This work was supported by the National Natural Science Foundation of China (10975150, 10775153) and the CAS Knowledge Innovation Program-"CSNS R&D Studies".

REFERENCES

[1] R. Aβmann, et al., An improved collimation system for LHC, Proc. of EPAC 2004, p.536-538

[2] D.E. Johnson, A dynamic dispersion insertion in the Fermilab main injector for momentum collimation, Proc. of PAC 2007, p. 1967

[3] J.B. Jeanneret, Optics of a two-stage collimation system, Phys. ST-AB, 1, 081001, (1998)

[4] C. M. Warsop, Beam Loss Control on the ISIS Synchrotron: Simulations, Measurements, Upgrades, Proc. of HALO 2003, pp. 154-157

[5] K. Yamamoto, Efficiency simulations for the beam collimation system of J-PARC/RCS, Phys. ST-AB, 11, 123501 (2008)

[6] S. X. Fang, S. N. Fu, Q. Qin, J. Y. Tang, S. Wang, J. Wei, and C. Zhang, J. Korean Phys., 48 (4), 697 (2006)

[7] J.Y. Tang et al., High-intensity aspects of CSNS accelerators, these proceedings

[8] S. Wang et al., these proceedings

[9] P.J. Bryant, E. Klein, The design of betatron and momentum collimation systems, CERN SL/92-40 (August, 1992)

[10] N. Catalan-Lasheras, On the use of thin scrapers for momentum collimation, Proc. of PAC 2001, Chicago, (2001), p.1520

[11] J. Wei, "Synchrotrons and accumulators for high-intensity proton beams", Reviews of Modern Physics, Vol. 75, No. 4, 1383 - 1432 (2003)

[12] U. Rohrer, PSI Graphic Turtle Framework based on a CERN-SLAC-FERMILAB version by K.L. Brown et al., 2006

[13] J. D. Galambos et al., ORBIT User Manual Version 1.10, July 1999

[14] N. Wang, these proceedings